Progress and Challenges in Phenomenological Determination of PDFs

Keping Xie



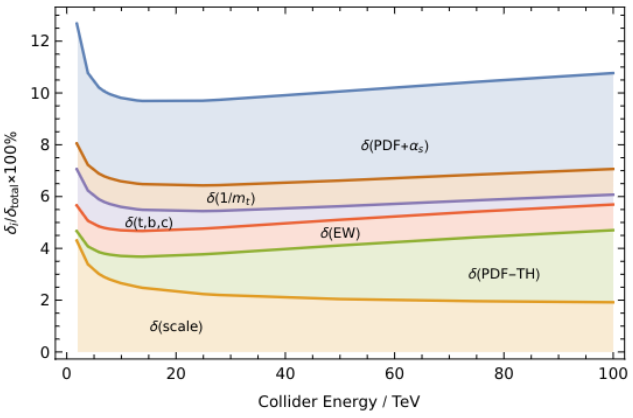
The 6th Chinese Lattice QCD Workshop

8–11 October 2026

The Chinese University of Hong Kong, Shenzhen

On behalf of the CTEQ-TEA (Tung Et Al.) Collaboration

Precision collider physics needs reliable PDFs

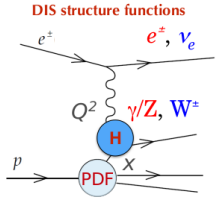


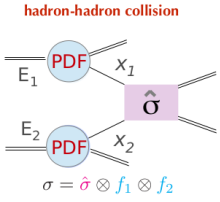
- PDF uncertainty limits Higgs and electroweak precision.
- Lattice QCD adds independent information on weakly constrained PDF combinations.

CT25 represents the latest progress in phenomenological determinations of precision PDFs.

Illustrative Higgs uncertainty budget from the 2022 Snowmass study, arXiv:2203.13923.

Collinear factorization separates the calculable hard scattering





$$F_a(x, Q^2) = \sum_i C_{a,i} \otimes f_i + \mathcal{O}(\Lambda^2_{\rm QCD}/Q^2),$$

$$\sigma_{pp\to X} = \sum_{ij} f_i \otimes f_j \otimes \hat{\sigma}_{ij\to X}.$$

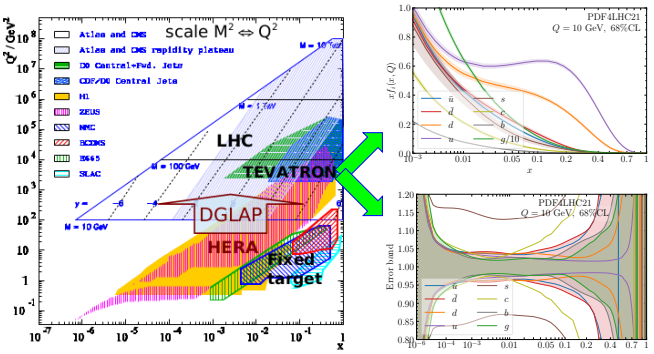
- Hard coefficients: perturbative QCD, with a specified order and scheme.
- PDFs: universal hadronic matrix elements, inferred from data.
- Scale dependence follows DGLAP evolution:

$$\frac{\partial f_i(x,\mu^2)}{\partial \ln \mu^2} = \sum_j P_{ij} \otimes f_j(x,\mu^2).$$

Collins, Soper and Sterman, factorization review (1989). PDF review: arXiv:1709.04922.

A global PDF fit is an inverse problem with physical constraints

Forward: PDFs $\longrightarrow$ cross sections **Inverse:** measured cross sections $\longrightarrow$ PDFs



- Parametrize $f_i(x, Q_0; a)$ and evolve with DGLAP.
- Finite data constrain convolutions over limited kinematics.
- Test PDF shapes, theory choices and uncertainty prescriptions.

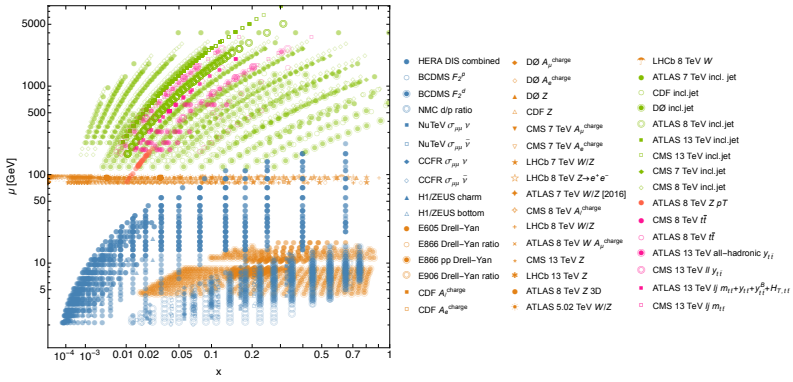
Fit correlated measurements

$$\chi^2(a) = [D - T(a)]^T \, C^{-1} [D - T(a)].$$

Sum rules: $\int_0^1 (u - \bar{u})\, dx = 2, \quad \int_0^1 (d - \bar{d})\, dx = 1, \quad \sum_i \int_0^1 x f_i(x, Q_0)\, dx = 1.$

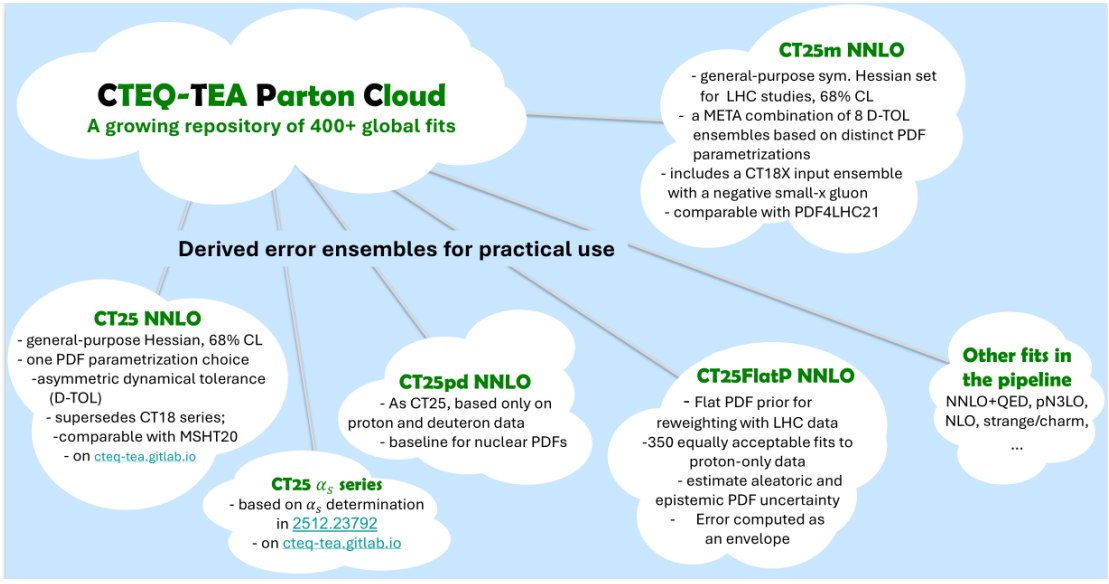
Illustrative fit diagram; PDF4LHC21 panels at $Q = 10$ GeV, 68% CL, arXiv:2203.05506. Schematic Gaussian likelihood.

Global data cover a broad but incomplete kinematic range



- DIS anchors the quark sea and scaling violations. LHC data add high-scale flavor and gluon information.
- Coverage weakens near $x \to 1$ and below the fitted small-x region, where error bands depend on fit assumptions.

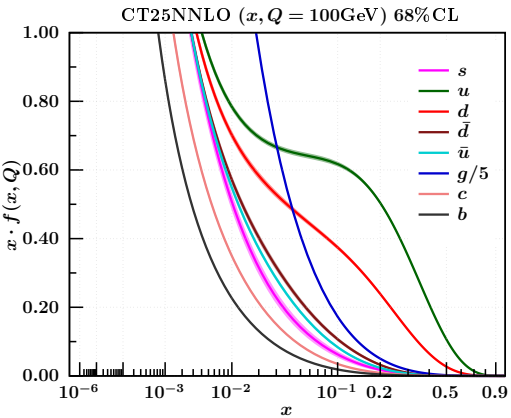
CT25 study, CTEQ-TEA (2026). Point locations represent process-dependent estimates of PDF sensitivity.



Parton Cloud: P. Nadolsky, DIS2026 (snapshot). CTEQ-TEA PDF catalogue.

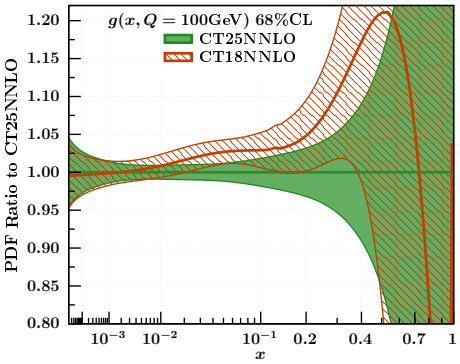
CT25: latest progress in precision PDF determination

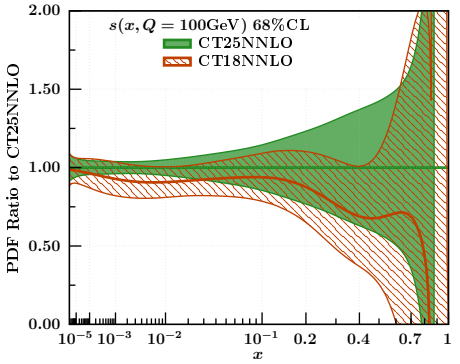
- NNLO Hessian PDFs with 68% CL uncertainties.
- Asymmetric dynamical tolerance.
- Thirteen precision LHC data sets: Drell–Yan, jets and $t\bar{t}$.
- SeaQuest Drell–Yan flavor data.
- More than 300 fits test parametrizations and methods.



CT25 study, CTEQ-TEA (2026). Public sets: CTEQ-TEA PDF catalogue. Progress proceedings: arXiv:2512.19779.

CT25 shifts the gluon and strange sea within the earlier uncertainty

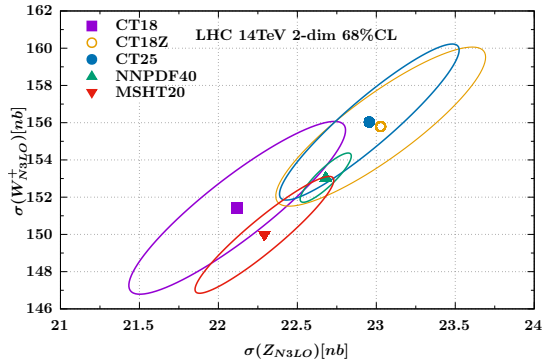


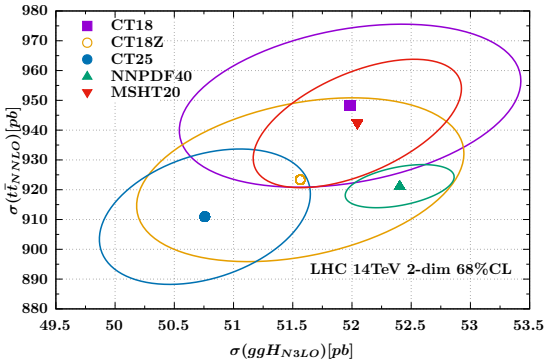


- LHC jet data favor a softer gluon for $x \gtrsim 10^{-2}$ in this analysis.
- Precision Drell–Yan data favor a larger strange distribution.
- The baseline also removes CCFR/CDHSW inclusive neutrino–nucleus DIS. New data and tolerance choices affect the band widths.

CT25 study, CTEQ-TEA (2026). Interpret each band using its indicated confidence convention.

CT25 predictions connect PDF progress to collider precision

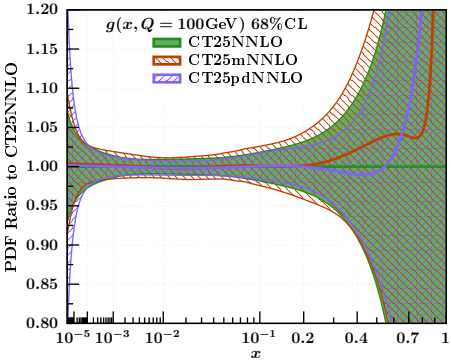


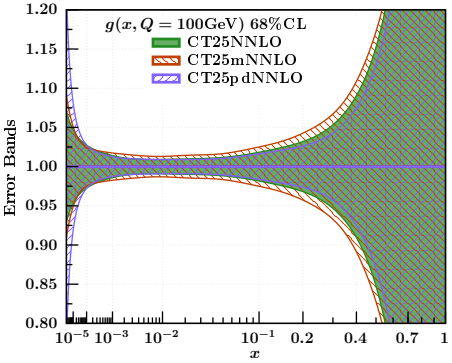


- CT25 predictions broadly agree with earlier fits; shared PDFs correlate the cross sections.
- Data choices and uncertainty prescriptions affect ellipse sizes and orientations.
- Use the correlations when comparing rates, ratios, or the impact of new constraints.

CT25 study, CTEQ-TEA (2026). Ellipse conventions follow the figure labels.

CT25m: combining alternative fits for LHC predictions

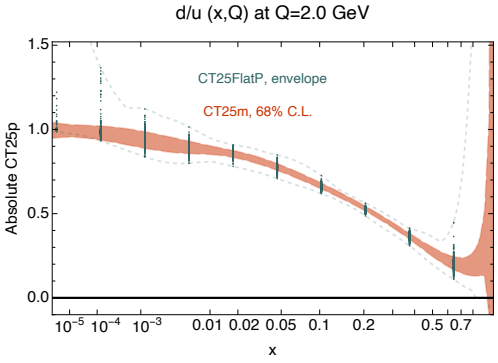


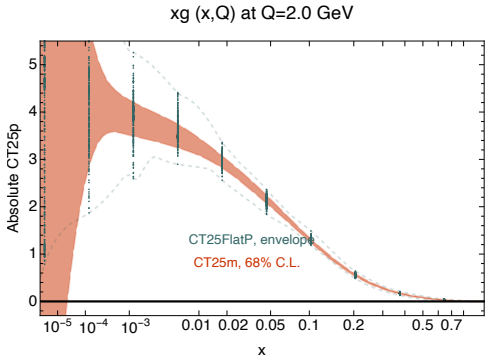


- META combination of eight dynamical-tolerance ensembles with distinct parametrizations.
- General-purpose symmetric Hessian set for LHC studies: 40 error directions, 68% CL.
- Incorporates between-fit spread; designed for comparisons with PDF4LHC21.

CT25 study, CTEQ-TEA (2026); official PDF catalogue. Gluon comparisons at $Q = 100$ GeV; band conventions follow the labels.

CT25FlatP makes the spread of acceptable fits visible

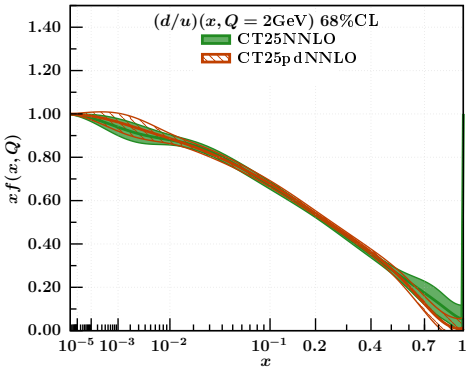


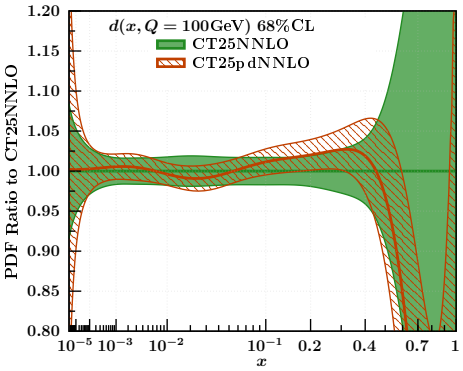


- CT25FlatP collects 350 acceptable proton-only fits and reports their envelope.
- The envelope illustrates sensitivity to fitting choices; it has a different meaning from a 68% interval.
- Lattice constraints should be tested across flexible fits as well as within a single parametrization.

CT25 study, CTEQ-TEA (2026). Plots compare the CT25FlatP envelope with CT25m 68% bands at $Q = 2$ GeV.

CT25pd: a proton/deuteron baseline for flavor separation

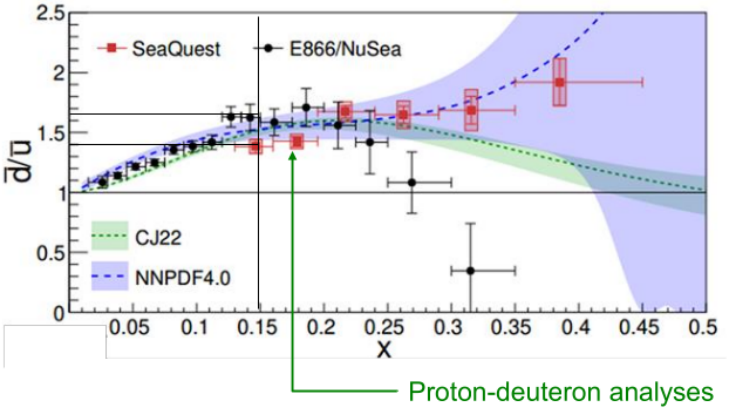




- CT25pd uses only proton/deuteron data: a baseline for nuclear PDF analyses.
- Deuteron DIS separates d from u; CJ–CT binding corrections affect the result.
- Reduced heavy-nucleus dependence still leaves deuteron and data-selection assumptions.

CJ–CT study: arXiv:2102.01107. CT25pd study, CTEQ-TEA (2026).

Light-antiquark asymmetry: $\bar{d}/\bar{u}$ probes the proton sea



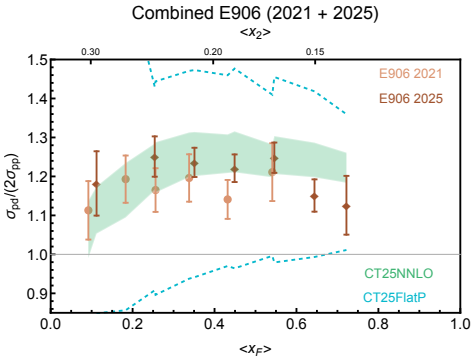
Leading-order forward Drell–Yan limit:

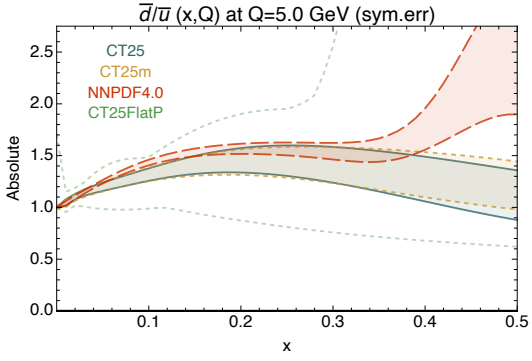
$$\frac{\sigma_{pd}}{2\sigma_{pp}} \simeq \frac{1}{2}\left[1 + \frac{\bar{d}(x_2)}{\bar{u}(x_2)}\right].$$

- Beam u dominance, isospin symmetry, negligible nuclear corrections.
- SeaQuest supports $\bar{d} > \bar{u}$ over its measured range.
- Fit cross sections with a consistent nuclear treatment.

SeaQuest: arXiv:2103.04024 (2021); arXiv:2512.17564 (final: $0.13 < x < 0.45$). Comparison from the supplied CT25 slides.

SeaQuest: cross sections and the inferred $\bar{d}/\bar{u}$

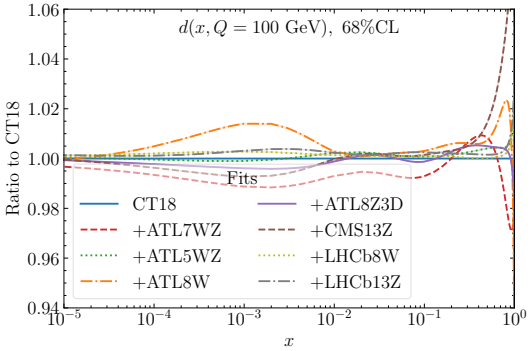


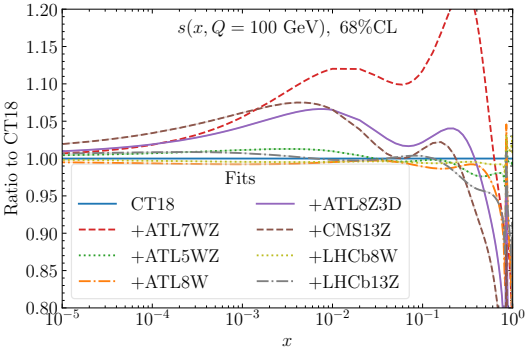


- CT25 fits the 2021 SeaQuest input. CT25FlatP excludes SeaQuest.
- Final data test updated cross-section predictions; they overlap the earlier sample.
- Different large-x extrapolations can agree with measured ratios yet differ in $\bar{d}/\bar{u}$.

Preliminary CT25-family comparisons, CTEQ-TEA (2026). Final data: arXiv:2512.17564.

Precision Drell–Yan data reveal tensions in flavor separation

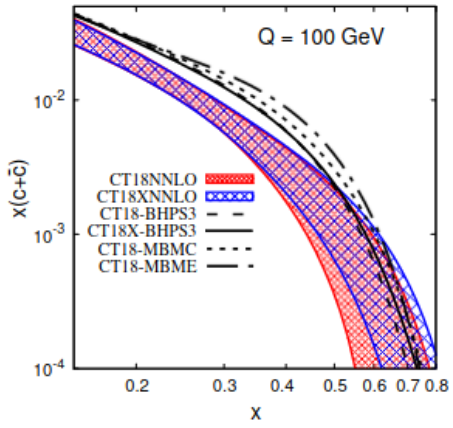




- Several new Drell–Yan data sets favor enhanced strangeness in CT18-based fits.
- The ATLAS 8 TeV W data give a different pull on d and $\bar{d}$.
- Flexibility can accommodate some shifts, while tensions remain in the combined fit.

CT18-based single-data-set studies, arXiv:2305.10733. These figures diagnose the inputs to CT25.

Intrinsic charm: testing the perturbative boundary condition



A valence-like charm component can arise from higher Fock states:

$$|p\rangle = a_{3q}|uud\rangle + a_{5q}|uudc\bar{c}\rangle + \cdots .$$

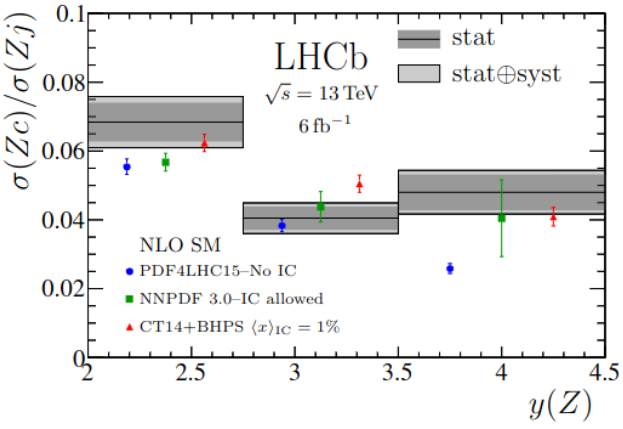
Schematically, in a specified matching scheme,

$$c(x,\mu) \simeq c_{\rm pert}(x,\mu) + c_{\rm fitted}(x,\mu).$$

- A fitted component tests the perturbative-charm boundary condition.
- Interpreting it as intrinsic charm depends on matching, higher orders and model assumptions.

CT18 fitted charm: arXiv:2211.01387. The charm decomposition is schematic and scheme dependent.

Forward $Z + c$ production probes the charm distribution



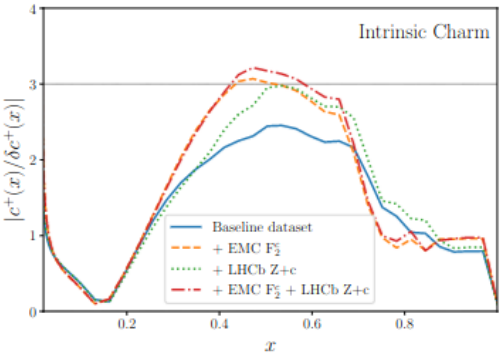
$gc \to Zc$ probes charm, with

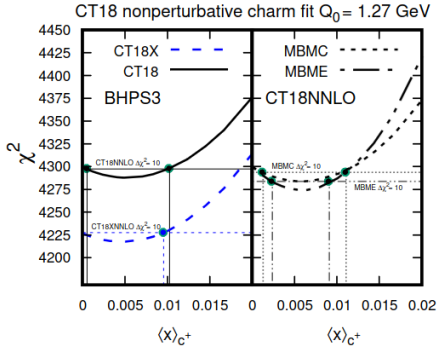
$$x_{1,2} \sim \frac{M_T}{\sqrt{s}} e^{\pm y}.$$

- Forward events enhance sensitivity to a large-x charm component.
- The charm-tagged fraction reduces some common rate uncertainties.
- Charm tagging, final-state radiation and shower matching affect the comparison.

LHCb $Z + c$: arXiv:2109.08084. CT14 intrinsic-charm phenomenology: arXiv:1707.00657. Kinematic estimate is schematic for a multibody final state.

Intrinsic-charm evidence depends on the inference prescription





- NNPDF reported 3σ evidence in its fitted-charm analysis.
- CT18FC finds a mild preference, compatible with zero under its uncertainty prescription.
- Resolving the difference requires controlled comparisons and additional charm-sensitive data.

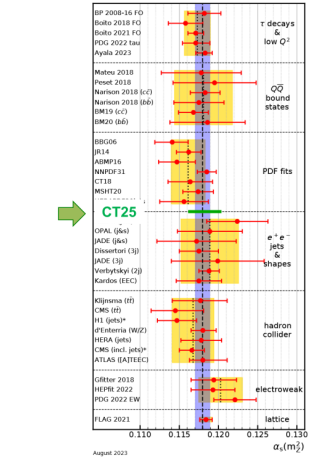
NNPDF: arXiv:2208.08372. CT18FC: arXiv:2211.01387. The two figures use different confidence constructions.

Where do we stand? Open challenges

- **Precision:** PDF errors limit M_W, the weak mixing angle and Higgs rates; inter-fit spread can exceed individual error bands.
- **Data:** correlated systematics and tensions, including ATLAS 7 TeV W/Z versus 8 TeV W, affect s and $d(\bar{d})$.
- **Methodology:** tolerance, parametrization and sampling bias; test coverage and stability under data-selection changes.
- **Theory:** N^{3}LO, electroweak corrections and the photon PDF; correlated scale and heavy-flavor uncertainties.
- **Proton structure:** large-x $\bar{d}/\bar{u}$, intrinsic charm and strangeness need independent constraints.
- **Extreme kinematics:** small-x resummation and saturation; forward charm/neutrinos at LHCb, FASER and a proposed FPF.

Precision, uncertainty and data tensions: arXiv:2203.13923, arXiv:2205.10444, arXiv:2305.10733. Forward Physics Facility proposal: arXiv:2203.05090.

α_s: CT25 in the PDG comparison



$\alpha_s(m_Z^2) = 0.1180 \pm 0.0009$ (PDG 2023 average).

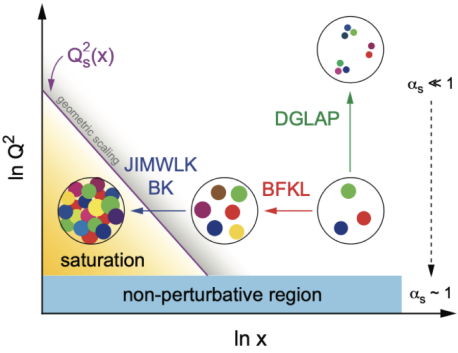
CT25: four uncertainty prescriptions

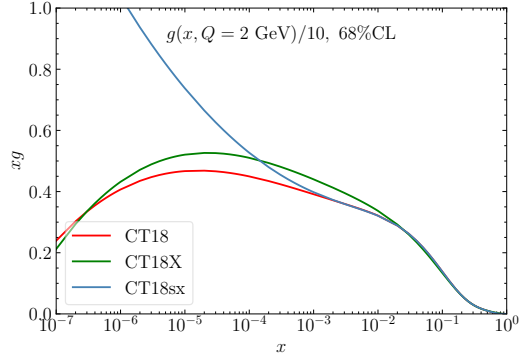
Method	$\alpha_s(M_Z)$
Global tolerance	$0.1184^{+0.0026}_{-0.0028}$
Dynamical tolerance	$0.1184^{+0.0024}_{-0.0012}$
Bayesian hierarchical (BHM)	$0.1181^{+0.0022}_{-0.0023}$
Gaussian mixture (GMM)	$0.1183^{+0.0023}_{-0.0023}$
Combination	$0.1183^{+0.0023}_{-0.0020}$

- CT25 (68% credibility) agrees with the **PDG 2023** average, 0.1180 ± 0.0009.
- Uncertainty shapes and widths depend on the inference method.

PDG 2023 compilation, with CT25 annotation. CT25: arXiv:2512.23792; mixture model: arXiv:2406.01664.

Small-x PDFs: theory choices and extrapolation





- CT18sx: NNLO+NLLx resummation changes evolution through enhanced $\ln(1/x)$ terms.
- CT18X: saturation-inspired DIS scale choice; it does not implement nonlinear evolution.
- Very small x is weakly constrained; F_L, forward charm and neutrinos can test extrapolations.

Left: schematic of small-x dynamics. Right: illustrative CT18-based gluon comparison at $Q = 2$ GeV, 68% CL. Preliminary CT18sx study: arXiv:2108.06596; CT18X: arXiv:1912.10053. Linear resummation and nonlinear saturation are distinct.

Towards N^{3}LO PDFs: a consistent theory upgrade

$$\frac{df}{d\ln\mu^2} = \left[a_s P^{(0)} + a_s^2 P^{(1)} + a_s^3 P^{(2)} + a_s^4 P^{(3)}\right] \otimes f, \qquad a_s = \frac{\alpha_s}{4\pi}.$$

Ingredient	Progress and remaining work
Four-loop evolution	Exact non-singlets (2026); singlet approximations use moments and endpoint limits.
DIS and heavy flavors	Massless coefficients through α_s^3; approximate massive terms and consistent threshold matching.
Hadronic fit inputs	Incomplete N^{3}LO coverage: document lower-order inputs and approximations.
Theory uncertainty	Correlate approximation errors and missing higher orders.

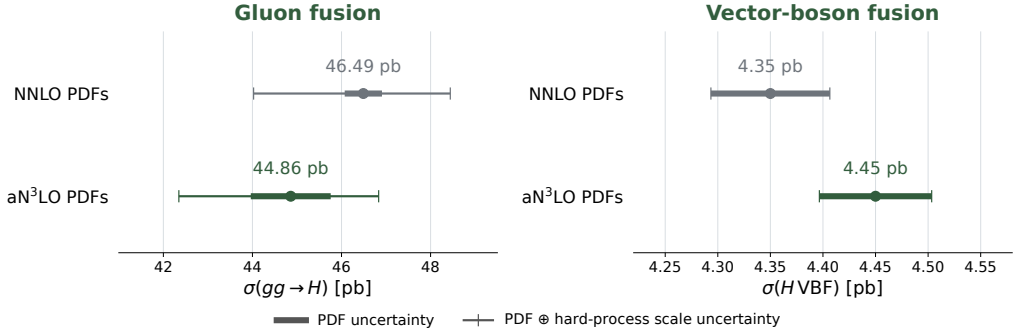
Fit uncertainty: MSHT nuisance parameters; NNPDF theory covariance matrices.

Higher-order evolution alone does not define a complete N^{3}LO global fit.

MSHT: arXiv:2207.04739; NNPDF: arXiv:2402.18635. Four-loop progress: arXiv:2604.09534, arXiv:2609.34837. Status: October 2026.

Towards N^{3}LO PDFs: the impact on Higgs predictions

MSHT20×NNPDF4.0 combinations, pure QCD; $\sqrt{s} = 13.6$ TeV. Hard calculations fixed at N^{3}LO.



- MSHT and NNPDF provide public aN^{3}LO fits and combined PDF sets.
- PDF-order changes shift the predicted Higgs rates by several percent.
- CTEQ-TEA: CT25 NNLO $\longrightarrow$ partial N^{3}LO benchmarks and fit development.

Higgs benchmark: Cridge et al., arXiv:2411.05373 (2025), Table 1; outer bars: PDF ⊕ 7-point scale error. CTEQ-TEA: arXiv:2512.19779.

Lattice input in phenomenological PDF fits

Euclidean matrix elements $\longrightarrow$ renormalization and matching

$f_i^{\overline{\rm MS}}(x,\mu)$ $\longrightarrow$ constraints in a global fit

Strange asymmetry: $s_-(x) = s(x) - \bar{s}(x)$

LaMET quasi-PDF approach.

Weakly constrained $s - \bar{s}$ with $\int_0^1 (s-\bar{s})\,dx = 0$.

CT18As $\longrightarrow$ CT18As_Lat.

Gluon: $g(x)$

Pseudo-PDF / Ioffe-time approach.

Adds large-x information complementary to collider jets.

CT18 / CT18As $\longrightarrow$ fits with lattice input.

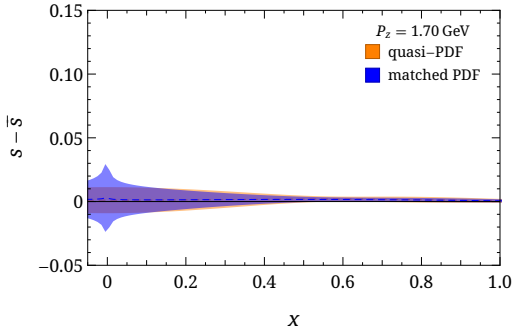
- Direct lattice input in both studies covers $0.3 \le x \le 0.8$; the gluon study also tests $0.4 \le x \le 0.7$.
- These lattice studies use CT18-based fits, distinct from the CT25 results shown earlier.

A common PDF definition connects lattice QCD, global fits, and collider predictions.

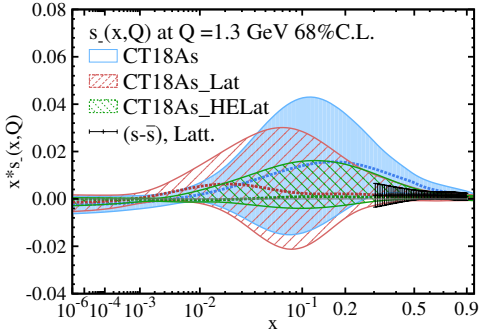
Hou, Lin, Yan and Yuan, arXiv:2211.11064; Ablat, Dulat, Hou, Lin, Xie and Yuan, arXiv:2502.10630.

Lattice input narrows the allowed strange asymmetry

Matched lattice input



Global-fit response at $Q_0 = 1.3$ GeV

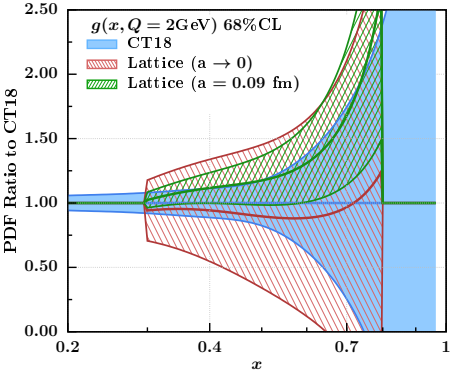


- The lattice constraint narrows the large-x $s - \bar{s}$ band in CT18As_Lat.
- One spacing ($a = 0.12$ fm), extrapolated to physical pion mass, $P_z \simeq 1.7$ GeV: systematic control remains crucial.
- **HELat halves lattice errors (projection).** Small-x gains depend on parametrization.

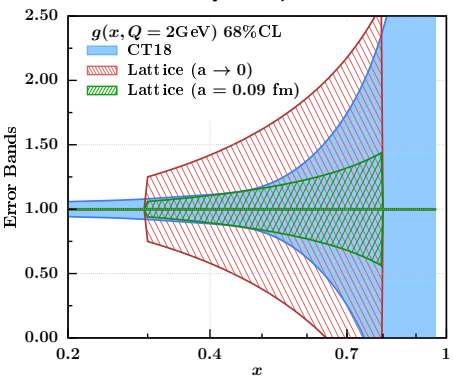
Hou et al., arXiv:2211.11064, Figs. 1 and 4. Right: 68% CL global-fit bands; lattice fit input restricted to $0.3 \leq x \leq 0.8$.

Gluon constraints depend on control of lattice systematics

Central values relative to CT18



Uncertainty comparison

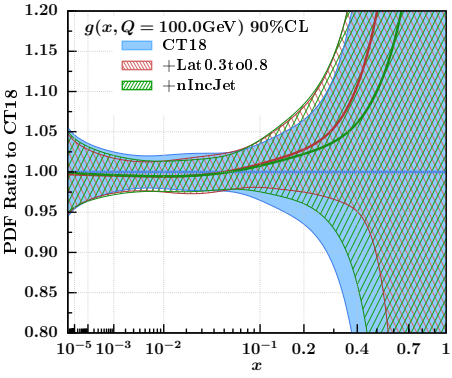


- Physical-continuum input: broad errors give negligible impact on the global fit.
- The $a \simeq 0.09$ fm, $m_\pi \simeq 310$ MeV ensemble illustrates possible future precision.

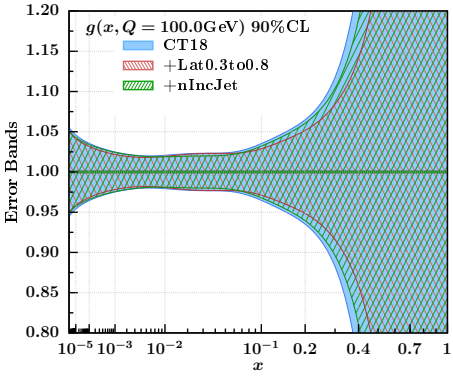
Ablat et al., arXiv:2502.10630, Fig. 2; input at $Q = 2$ GeV, bands at 68% CL. Stronger effects on the next two slides use the single-ensemble scenario.

Lattice information complements the jet constraint on the gluon

Change in the central gluon PDF



Change in the uncertainty band

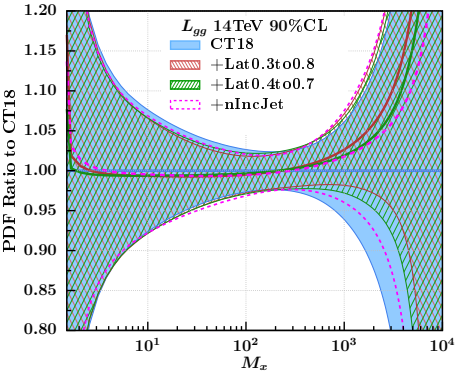


- Single-ensemble lattice input and selected jets both harden the CT18 large-x gluon.
- The all-jet comparison finds broader jet coverage; lattice is competitive at $x \gtrsim 0.5$.

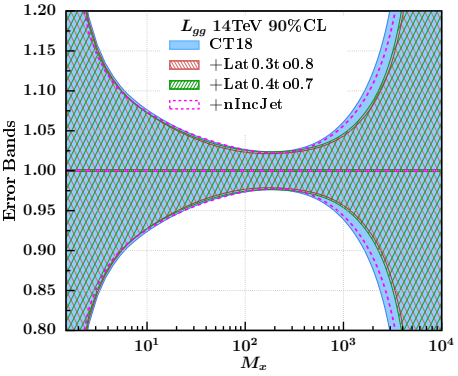
Ablat et al., arXiv:2502.10630, Figs. 9–10 and Sec. III.B; $Q = 100$ GeV, 90% CL. Illustrative single-ensemble lattice input. nIncJet: ATLAS 8/13 TeV and CMS 13 TeV inclusive jets.

Large-x lattice information propagates to high-mass predictions

gg luminosity, 14 TeV; M_X in GeV



Relative PDF uncertainty



- The single-ensemble scenario enhances high-mass gg luminosity and narrows its PDF uncertainty.
- Next steps: control systematics, publish covariance information, test matching and fit flexibility.

Ablat et al., arXiv:2502.10630, Fig. 11; 90% CL. Illustrative single-ensemble lattice input. Implications for global-fit practice are the synthesis of these two case studies.

Priorities for lattice input in precision PDF fits

Priority	Information needed for a combined analysis
Controlled systematics	Continuum and physical-mass limits; finite-momentum effects; matching and reconstruction stability
Defined fit domain	Scale, scheme, normalization, and a justified x range with variations of the endpoints
Correlations	Covariance information or correlated replicas, with identifiable statistical and systematic components
Joint validation	Flexible PDF shapes, alternative experimental baselines, and tests of predictions outside the fitted input

Resolve a weakly constrained PDF direction while demonstrating control of bias.

Proposed priorities motivated by the strange-asymmetry and gluon studies: arXiv:2211.11064 and arXiv:2502.10630.

Precision PDFs and the lattice opportunity

- **CT25** represents the latest progress in phenomenological determinations of precision PDFs, supported by the CTEQ-TEA Parton Cloud.
- **Remaining challenges:** data tensions, theory and fit choices; flavor structure and small-x extrapolation need independent constraints.
- **Lattice opportunity:** strange asymmetry and the large-x gluon provide concrete targets for independent constraints.
- **Next step:** advance toward N^{3}LO fits, combine controlled lattice inputs with data, and validate the resulting PDF uncertainties.

Thank you

Backup: strange moments and global-fit quality

$$s_\pm = s \pm \bar{s}, \quad \langle x^n \rangle_{s_\pm} = \int_0^1 dx\, x^n s_\pm(x, Q).$$

Quantity	CT18A	CT18As	CT18As_Lat
$\chi^2_{\rm exp}$ (3674 points)	4376	4344	4361
$\langle x \rangle_{s_-}$, $Q = 1.3$ GeV	0	0.0074 ± 0.0112	0.0016 ± 0.0070
$\langle x^2 \rangle_{s_-}$, $Q = 1.3$ GeV	0	0.0024 ± 0.0027	0.00057 ± 0.00120
$\langle x \rangle_{s_+}$, $Q = 2$ GeV	0.043 ± 0.010	0.052 ± 0.017	0.048 ± 0.016

- These are fit-derived moments with 68% CL uncertainties; $\chi^2_{\rm exp}$ excludes lattice input.
- Local-lattice determinations of $\langle x \rangle_{s_+}$ at 2 GeV:
  ETMC: 0.052 ± 0.012; χQCD: $0.051 \pm 0.026 \pm 0.005$.
- Traditional local-operator moments include $\langle x \rangle_{s_+}$ and $\langle x^2 \rangle_{s_-}$; $\langle x \rangle_{s_-}$ above is inferred from the fitted x dependence.

Hou et al., arXiv:2211.11064, global-fit comparison and moment table. Lattice moment results are quoted there from ETMC and χQCD.

The CT25 family separates application-specific uncertainty choices

Ensemble	Construction	Intended use
CT25	Asymmetric Hessian with dynamical tolerance, 68% CL	General-purpose proton predictions
CT25pd	Proton/deuteron data with a deuteron correction	Baseline with reduced heavy-nucleus dependence
CT25m	Symmetric META combination of alternative fits, 68% CL	LHC predictions including a broader fit spread
CT25FlatP	Envelope of 350 acceptable proton-only solutions	Sensitivity to fit choices and reweighting studies

The FlatP envelope has a different meaning from a 68% Hessian interval.

CT25 study and official CTEQ-TEA PDF catalogue.

New precision data sharpen flavor and gluon constraints

Process	Added information	Published input studies
LHC Drell–Yan	W/Z rapidity distributions at 5.02, 8 and 13 TeV	arXiv:2305.10733
LHC $t\bar{t}$	Differential rapidity and mass spectra	arXiv:2307.11153
LHC jets	Inclusive jet and dijet spectra	arXiv:2412.00350
SeaQuest	Proton/deuteron Drell–Yan ratio at large x	Final data: arXiv:2512.17564

Precision makes correlated systematics and theory choices more consequential.

CT25 fits the 2021 SeaQuest data. The final SeaQuest data provide a later comparison.

A good global χ^2 can coexist with poorly described data sets

Data set	$N_{\rm pt}$	CT18	CT18A	CT18As
ATLAS 5.02 TeV W/Z	27	0.89	0.70	0.70
ATLAS 8 TeV W	22	2.75	2.94	2.79
CMS 13 TeV Z	12	2.45	2.02	1.73
ATLAS 7 TeV W/Z	34	2.59	2.51	2.31
Global fit		1.20	1.20	1.19

All numeric entries in the last three columns are $\chi^2/N_{\rm pt}$.

- CT18As adds freedom to the strange parametrization.
- The global average dilutes local tensions because other experiments dominate the point count.

Illustrative CT18-family refits from the CT25 study, based on arXiv:2305.10733. These are not CT25 fit-quality values.

Tolerance and validation address different parts of the inference problem

Hessian uncertainty

$$\chi^2(a) \simeq \chi^2_{\min} + \sum_k z_k^2, \qquad \Delta\chi^2 = T_k^2.$$

- $T = 1$ follows an ideal local Gaussian model.
- Global or dynamical tolerances account for broader compatibility criteria.
- Published confidence conventions differ among PDF sets.

Validation beyond a local minimum

- Closure tests probe recovery of known pseudo-data truth.
- Fits to subsets test stability and prediction of withheld measurements.
- Alternative parametrizations test dependence on the chosen function space.
- Lagrange-multiplier scans test nonquadratic directions.

CT18: arXiv:1912.10053. NNPDF4.0: arXiv:2109.02653. Uncertainty study: arXiv:2205.10444.

Backup: Hessian and Monte Carlo PDF errors

$$\Delta X_{\mathrm{H}} = \frac{1}{2}\sqrt{\sum_{k=1}^{N_{\mathrm{eig}}}\left(X_k^+ - X_k^-\right)^2}, \qquad \Delta X_{\mathrm{MC}} = \sqrt{\frac{1}{N_{\mathrm{rep}}-1}\sum_{r=1}^{N_{\mathrm{rep}}}\left(X_r - \overline{X}\right)^2}.$$

- Hessian eigenvector sets probe fitted directions; Monte Carlo replicas sample a distribution.
- These are symmetric standard-deviation formulas; use the provider's prescription for asymmetric bands and nonlinear observables.
- A Gaussian 90% interval converts to 68% by dividing by 1.645. Check the set's confidence level and tolerance convention before converting or comparing.

CT18: arXiv:1912.10053; PDF4LHC21 combination and prescriptions: arXiv:2203.05506.

Backup: nuisance profiling and multiplicative systematics

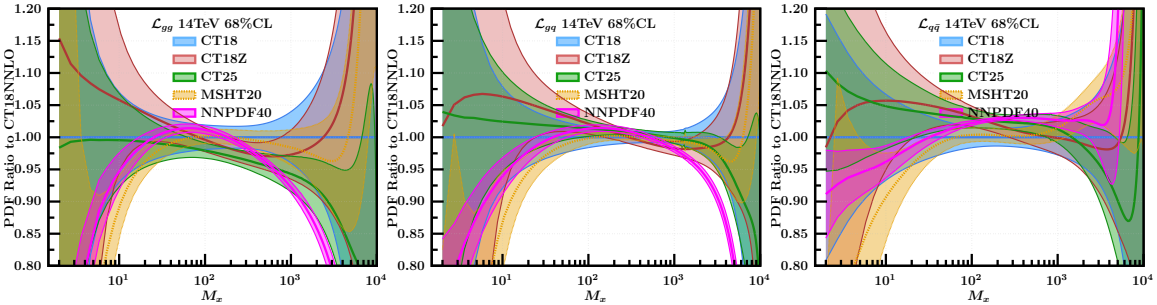
$$\chi^2(\boldsymbol{a}, \boldsymbol{r}) = \sum_i \frac{\left[D_i - T_i(\boldsymbol{a}) - \sum_\alpha \beta_{i\alpha} r_\alpha\right]^2}{s_i^2} + \sum_\alpha r_\alpha^2, \qquad \chi^2_{\rm prof}(\boldsymbol{a}) = \min_{\boldsymbol{r}} \chi^2.$$

- s_i: uncorrelated errors; r_α: correlated shifts with Gaussian penalties.
- For multiplicative errors, use a theory-based reference, $\beta_{i\alpha} = \epsilon_{i\alpha} T_i^{\rm ref}$, with a consistently specified or iterated prescription.
- Scaling relative errors by fluctuating data values can bias a normalization fit; inspect fitted shifts as well as the total χ^2.

CT18 methodology: arXiv:1912.10053; precision Drell–Yan study: arXiv:2305.10733.

Parton luminosities translate PDF differences into collider rates

$$\frac{d\mathcal{L}_{ij}}{d\tau} = \int_\tau^1 \frac{dx}{x}\, f_i(x,\mu^2) f_j(\tau/x,\mu^2), \qquad \tau = \frac{M_X^2}{s}.$$



Broad agreement among global sets still allows process-dependent differences.

Ordered luminosity definition. CT25 study, CTEQ-TEA (2026).

Backup: selected references

- **CT25:** CTEQ-TEA public PDF catalogue; progress proceedings, arXiv:2512.19779.
- **Global-fit framework:** CT18, arXiv:1912.10053.
- **Approximate N^{3}LO:** MSHT, arXiv:2207.04739; NNPDF, arXiv:2402.18635; combination, arXiv:2411.05373.
- **Sea asymmetry and deuteron corrections:** SeaQuest, arXiv:2512.17564; CJ–CT, arXiv:2102.01107.
- **Intrinsic charm:** NNPDF, arXiv:2208.08372; CT18FC, arXiv:2211.01387; LHCb $Z + c$, arXiv:2109.08084.
- **Lattice strange asymmetry:** Hou, Lin, Yan and Yuan, arXiv:2211.11064.
- **Lattice gluon:** Ablat, Dulat, Hou, Lin, Xie and Yuan, arXiv:2502.10630.
- **Uncertainty and strong coupling:** arXiv:2205.10444; arXiv:2512.23792.
- **LHC input studies:** Drell–Yan, arXiv:2305.10733; top, arXiv:2307.11153; jets, arXiv:2412.00350.